ADVANCED OPTICAL MATERIALS
www.advopticalmat.de

Observation of Binary Spectral Jumps in Color Centers in Diamond

Zhao Mu, Yu Zhou, Disheng Chen, Johannes E. Fröch, Jianqun Yang, Xingji Li, Igor Aharonovich,* and Wei-Bo Gao**

Optical "blinking" normally refers to a switching behavior of fluorescence for quantum emissions between "ON" and "OFF" state. For quantum dots, single molecules, and nitrogen-vacancy centers in diamond, it usually stems from conversions between two different charge states, with one emitting strong and bright fluorescence while the other scattering weak or no fluorescence. Here, a different type of blinking from single emitters in ion implanted diamond is reported, with both blinking states exhibiting detectable photoluminescence under nonresonant excitation. Thanks to the low jumping rates, the dynamics of the emission can be directly monitored. The quadratic power dependence of the conversion rates suggests the possibility of two-photon ionization process in quantum jumps. This work provides extra insights into the photodynamics of the spectral jumps on defect-based single-photon emitters hosted in wide-bandgap semiconductors.

1. Introduction

Color centers in diamond are promising building blocks for a variety of quantum applications[1] including high-sensitive quantum metrology,[2] long-distance quantum communication,[3] and large-scale quantum computing.[4] Among them, nitrogen vacancy (NV) center in diamond has been heavily studied,[5] on which observation of transform-limited linewidth[6] and generation of indistinguishable photons from distinct emitters[7] have been realized. However, NV centers suffer from strong electron–phonon interaction causing a low Debye–Waller (DW) factor,[8] and high susceptibility to the fluctuation of electric field of local environment.[6,9] Recently, negatively charged split-vacancy color centers in diamond, such as silicon-vacancy (SiV)[10] and germanium-vacancy (GeV)[11] centers, have emerged as attractive quantum systems by exhibiting long spin coherence times[12] and superior optical properties.[13] These emitters scatter most light in zero-phonon line and exhibit low vulnerability to the electric-field fluctuations, as granted by the inversion symmetry of the molecular structures.[14] Together with the narrow inhomogeneous broadening, two-photon interference between two distinct SiV emitters on the same sample has been demonstrated without invoking any spectral tuning technique.[15]

However, emission intermittency[16] and spectral jumps[17] have also been reported on these quantum emitters when embedded in nanodiamonds or nanostructures. Much of efforts have been invested to understand the underlying physics and search for methods to overcome these problems.[18] Although similar phenomena have been reported and investigated on other low-dimensional systems, such as quantum dots, nanorods, and molecules,[16a,19] the exact photophysics involved in split-vacancy systems is expected to be different. For example, some types of these color centers exhibit a small spectral diffusion with a relatively narrow linewidth, thanks to its low sensitivity to the local electric-field fluctuations[20] while the others show a wide distribution of emission wavelengths which is accompanied by a clear bimodular photon statistics.[21] So far, a complete understanding of these phenomena is still lacking.

Here, we directly observe spectral jumps from single color centers in diamond under nonresonant excitation at cryogenic temperature. Simultaneous recording of fluorescence from both blinking states reveals a complete anticorrelation between two states that can unambiguously be associated with a single quantum emitter. Considering the stochastic nature of these processes, there must be only two of these states involved in the spectral jumps. Finally, the quadratic excitation power dependence of the jumping rates suggests a two-photon ionization process for conversions between the two states. Together with

Z. Mu, Dr. Y. Zhou, Dr. D. Chen, Prof. W.-B. Gao
Division of Physics and Applied Physics
School of Physical and Mathematical Sciences
Nanyang Technological University
Singapore 637371, Singapore
E-mail: wbgao@ntu.edu.sg
Dr. D. Chen, Prof. W.-B. Gao
The Photonics Institute and Centre for Disruptive Photonic Technologies
Nanyang Technological University
Singapore 637371, Singapore
J. E. Fröch, Prof. I. Aharonovich
School of Mathematical and Physical Sciences
University of Technology Sydney
Ultimo, NSW 2007, Australia
E-mail: igor.aharonovich@uts.edu.au
Prof. J. Yang, Prof. X. Li
School of Materials Science and Engineering
Harbin Institute of Technology
Harbin 150001, P. R. China
E-mail: lxj0218@hit.edu.cn
The ORCID identification number(s) for the author(s) of this article can be found under https://doi.org/10.1002/adom.202000495.

DOI: 10.1002/adom.202000495

previous works,[17c,22] our study proves that the fluorescence intermittency is an omnipresent phenomenon in solid-state quantum emitters, which at most times is related to an ionization process.

2. Experimental Results

2.1. Spectral Jumps

We characterized the optical properties of germanium implanted diamond sample at 20 K by using a home-built confocal microscope, as shown in **Figure 1**a. The sample was excited nonresonantly with either 532 nm continuous-wave (CW) light for count rate monitoring or 513 nm pulsed light for lifetime measurements. As a complementary study, we also investigated the spectral jumps of SiV color centers in nanodiamond by using resonant excitations. Details on sample preparations and experimental techniques can be found in the Experimental Section and Supporting Information.

The first color center (labeled as E1) investigated here exhibits a two-line structure that appears at two distinct wavelengths as indicated by red (state A) and blue (state B) in Figure 1b. We confirm that these two groups of spectral lines originate from the same quantum emitter by conducting a second-order correlation measurement, as shown in Figure 1c. During the measurement, a long-pass filter (>600 nm) was used for laser rejection while allowing for the detections of photons from all four transitions. We fit the data with the conventional second-order correlation function

$$g^{(2)}(\tau) = 1 - \alpha \times \exp\left(-|\tau| / \tau_{\text{dip}}\right) \quad (1)$$

where α and τ_{dip} represent the depth and the width of antibunching dip, respectively. Without further corrections to the finite instrument response time and APD dark counts, we obtain an antibunching dip as low as $g^{(2)}(0) = 0.19 \pm 0.02$, which verifies the quantum nature of the emitter and the single origin of all four spectral lines.

We note that the spectral jump between the two doublets is more than 47 meV, which is too wide to be accounted by the local electric-field fluctuations in the host material.[6,17b,23] Furthermore, the spectral splittings of the doublets are different from each other, specifically, 6.7 meV for the short-wavelength doublet and 11.6 meV for the long-wavelength pair. These observations imply that the two doublets should correspond to two different states of the same single emitter and the spectral jumps reflect the conversion processes between these two states. We associate the short-wavelength doublet (peak 1 and 2) to state A of the emitter, and the long-wavelength pair (peak 3 and 4) to state B, as shown in Figure 1b. By consecutively and continuously recording a series of spectra over time with an exposure time of 0.5 s per frame, we find no simultaneous

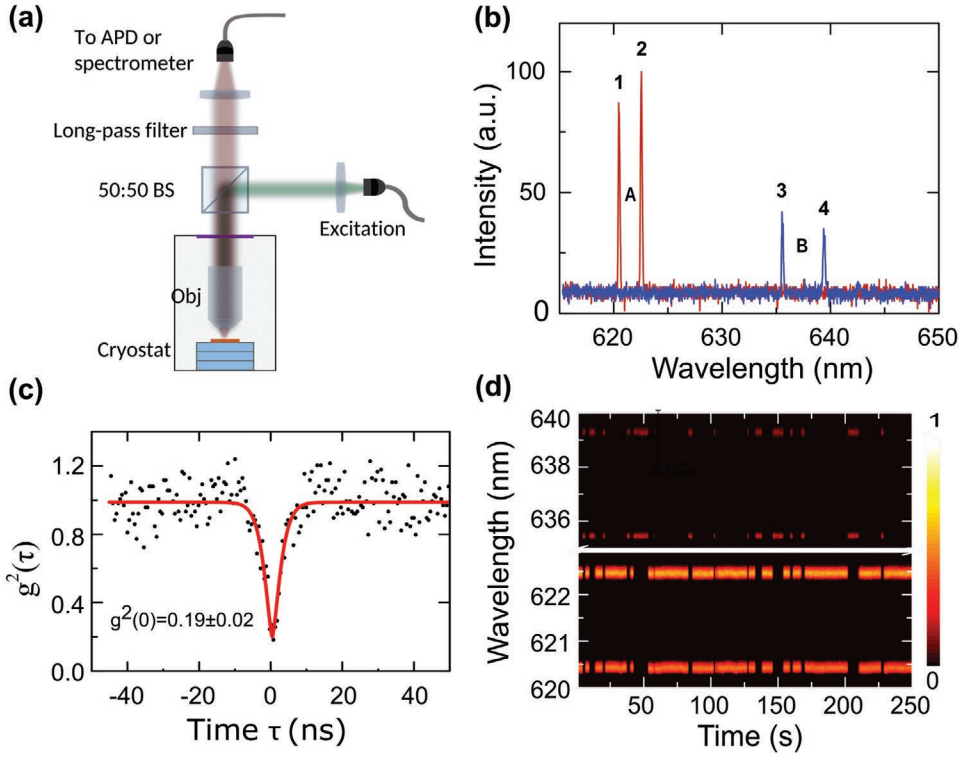

Figure 1. Spectral jump of emitter E1. a) Home-built confocal microscope with nonresonant excitation. b) Two PL spectra recorded at two different times, coded by red and blue, to illustrate spectral jumps. Both spectra are collected at 20 K with an integration time of 0.5 s. We associate peak 1 and 2 to state A, and peak 3, 4 to state B of the emitter. c) Second-order correlation function of the emitter at 20 K without any background correction. A long-pass filter at 600 nm is used in the collection path to suppress the laser reflection while allowing collecting PL from all four transitions. The depth of the antibunching dip, $g^{(2)}(0) = 0.19 \pm 0.02$, is extracted from a fitting (red line) by using Equation (1). d) Continuous and consecutive collection of 250 spectra, each exposed for 0.5 s. Clear and evident anticorrelation between the two fluorescence states A and B is observed.

detection of the two states in the data, as shown in Figure 1d. Such nearly complete anticorrelation between states A and B implies that only these two fluorescence states are involved in the observed spectral dynamics.

2.2. Lifetime and Temperature Dependence

Generally, the half width of an antibunching dip characterizes the dwell time of an emitter to scatter a second photon upon the emission of the first one, which in our case is $\tau_{dip} = 2.44 \pm 0.29$ ns. This value is consistent with the radiative lifetimes of both states A and B (see **Figure 2**a), suggesting a similar radiative quantum efficiency for both states when the emitter is driven by 532 nm nonresonant light.

More insight into the nature of these quantum emitters can be obtained from the temperature dependence of transitions, as shown in Figure 2b. As the temperature increases, all four transitions experience an evident broadening along with a decrease of radiative efficiencies due to the enhancement of phonon interactions. All peaks can be well fitted with a Lorentzian function whose center position and linewidth can be extracted and compared in Figure 2c. From 20 to 190 K, all lines exhibit a similar amount of homogeneous broadening of ≈4.2 meV, implying alike coupling strengths to the phonon bath of all transitions. In addition, peak 1 and 3 (peak 2 and 4) share a similar redshift of 1.4 meV (1 meV) as the temperature increases to 240 K, suggesting that the energy levels involved in transition 1 and 3 (or transition 2 and 4) may possess a similar electronic structure so as to respond similarly to the lattice vibrations and distortions as the temperature varies. Nevertheless, all four transitions exhibit a narrow linewidth of <0.6 meV at 20 K and display no evident phonon sideband up to 290 K.

2.3. ON and OFF Time Analysis

To obtain more insight into the underlying physics of the state conversion processes, we analyze the statistics of durations of photoluminescence (PL) intermittency of each state. Since the fluorescence intensity of state A is significantly stronger than B, we can determine the state of the emitter by monitoring the time resolved PL intensity, as shown in the inset of **Figure 3**a. We define a threshold of ≈90 kcps (the median of high 120 kcps and low 60 kcps) to extract the duration of ON period of state A followed by a histograming. These statistical occurrences are then cumulatively summed to give the occurrence that no conversion from A to B takes place within time t, or equivalently, the fluorescence is still ON after time t. Upon a normalization to the total number of conversion events, we obtain the probability to have the emitter reside in state A for at least a duration of t, as shown in Figure 3a. According to the quantum jump theory of incoherent excitation,[24] this probability should follow a single-exponential decay

$$P(t) = \exp(-R_{AB} \times t) \tag{2}$$

where R_{AB} is the conversion rate from state A to state B. Its inverse value corresponds to a characteristic time (τ_{AB}) at which a state conversion from A to B is likely to take place. For an excitation power of 0.846 mW, we find $\tau_{AB} = 1/R_{AB} = 4.03 \pm 0.02$ s (see Figure 3a). We note that these conversion processes are robust against temperature as shown in Figure S1 (Supporting Information).

As the excitation power increases, the conversion processes in both directions speed up (see Figure 3b,c). Particularly, the rates R_{AB} and R_{BA} follow quadratic functions over the power as $R = \beta P^2$ with coefficient β defining the conversion efficiency (see Figure 3d). The fact of $\beta_{BA} > \beta_{AB}$ indicates that state B should possess a higher energy with respect to state A, despite the lower emission energy than the latter. Due to the quadratic dependences of both rates, the emitter would always spend $\beta_{BA}/(\beta_{AB} + \beta_{BA})$ proportion of time in state A at equilibrium irrespective of the excitation power P. Here, we stress that the photoluminescence energy does not determine the energies of state A and B, which usually depends on the details of local environment such as the Fermi level, strains, and chemical components.

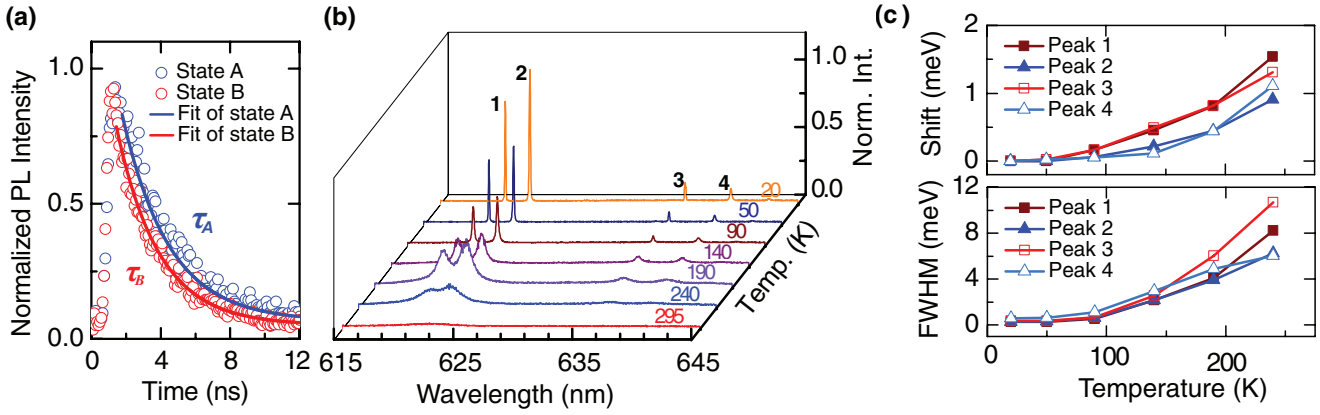

Figure 2. a) Excited state lifetimes of state A and B of the emitter E1 under 513 nm nonresonant pulsed excitation at an average power of 0.2 mW. The pulse is 80 ps long, repeating at 80 MHz. A band-pass filter of 620 ± 7 nm (640 ± 7 nm) is used to select the emission from state A (state B) for measurements. Solid lines are the fits with single exponential decay characterized by $\tau_A = 2.43 \pm 0.03$ ns and $\tau_B = 2.67 \pm 0.05$ ns, respectively. b) Temperature dependence of PL spectra, with an integration time of 15 s per line to ensure statistical recording of all four peaks. c) Center wavelength shift and FWHM of all four transitions extracted from Lorentzian fittings of spectra in (b).

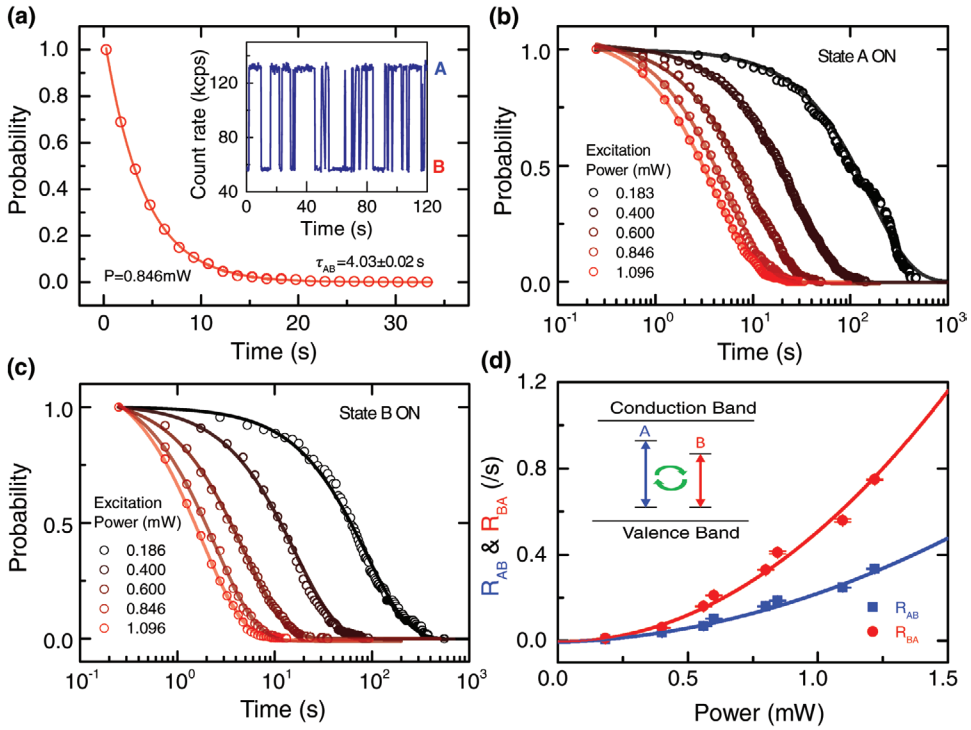

Figure 3. Statistics of spectral jumps of the emitter E1. a) Statistics of "ON" period for state A when the system is under 532 nm nonresonant excitation at a power of 0.846 mW. The dots are the raw data extracted from the fluorescence intensity over an acquisition period of ≈3 h. Solid line is the single exponential fit with a characteristic time of $\tau_{AB} = 4.03 \pm 0.02$ s. Inset: time-resolved fluorescence intensity recorded with 0.1 s binsize and 600 nm long-pass filter. The laser scattering and APD dark counts only account for ≈100 cps. b,c) Probability distribution of the duration of "ON" period for state A, and state B at different excitation powers. The solid lines are the single exponential fits. d) State conversion rates from A to B (R_{AB}) and from B to A (R_{BA}), found by inverting the characteristic times in (b) and (c). Solid lines are quadratic fit with $R = \beta P^2$, where P denotes the excitation power and β corresponds to the strength of conversion. Specifically, $\beta_{AB} = 0.24 \pm 0.02$ Hz mW^{-2} and $\beta_{BA} = 0.51 \pm 0.05$ Hz mW^{-2}. Inset: Schematic of possible conversion dynamics between the two states.

The quadratic power dependence is also reported on NV centers in diamond,[25] where a two-photon ionization process is proposed to account for the charge state conversions in the NV centers, i.e., between NV^- and NV^0.[17c,26] Similar physics might take place in our system as well: a nonresonant photon can promote an electron to the excited level of state A before getting "kicked" out of the emitter (into the conduction band of the host material) by interacting with a second photon. This leaves the emitter in the ground level of state B, as shown in the inset of Figure 3d. To return back to state A, the emitter can absorb an incident photon to promote the electron into the excited level of state B before acquiring a free electron from the valence band of the host material with the help of a second photon. This leaves the emitter in the ground level of state A.

2.4. Additional Emitters and Intensive Laser Exposure

Similar binary jumps have been verified on other two emitters (labeled as E2 and E3) in the same sample (see Figure S2a,d, Supporting Information). Unlike the doublet spectral lines of emitter E1, emitters E2 and E3 exhibit a single line structure at different energies as shown in **Figure 4**. The variations of emission energy and spectral structures can be attributed to the different local strains experienced by the different emitters, as shown in the SiV system.[27] Nonetheless, the on-off statistics follow a similar trend of exponential distribution as E1 (see Figure S2b, Supporting Information). Sometimes, the spectral jumps can be eliminated by exposing the color centers to an intense laser beam for a long period of time as shown in Figure S2c (Supporting Information). The resultant stabilized state usually shows different emission energies as comparing to the earlier jumping states. Specifically, for both emitters E2 and E3, the stabilized states show a sharp emission near 603 nm (see Figure 4b,c), almost identical to the 602 nm emission of GeV^- color centers, implying the Ge-related nature of these emitters.

We also investigated SiV color centers in nanodiamond to check if similar spectral jumps present in other group-IV emitters. Indeed, some emitters show binary jumps but with a jumping width of only a few GHz, as shown in Figure S3b,c (Supporting Information). This width is too small to be resolvable for a grating and we employ a novel resonant technique to monitor the jumping dynamics over time (details in Section S3, Supporting Information). Although the on-off period is also very long (see Figure S3d, Supporting Information), the mechanism of spectral jumps could be different from those of Ge-related emitters given the orders of magnitude difference in jumping energies. We stress that all color centers investigated in this work do not show evident bleaching or fluorescence reduction within the period of experiments.

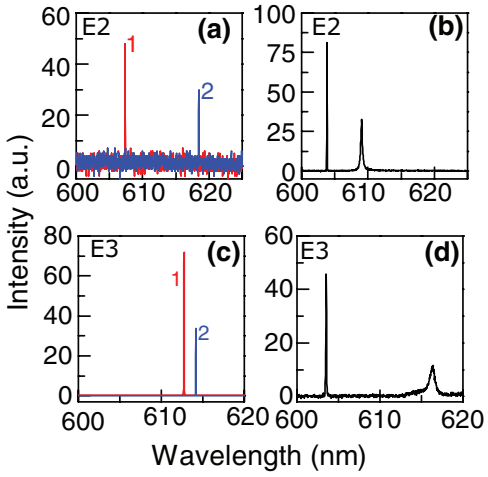

Figure 4. Two additional emitters showing spectral jumps. a) Spectral jumps of an emitter E2 between state "1" (607.3 nm) and state "2" (618.5 nm) under 0.5 mW 532 nm excitation, taken with an exposure time of 0.5 s per frame. b) Spectrum of the emitter E2 after a long-term (30 min) and intensive laser exposure (2 mW), with two peaks at 603.8 and 609.1 nm, respectively. The spectrum, acquired for 15 s, is normalized to 0.5 s for comparison. c) Spectral jumps of Emitter E3 between state "1" (612.7 nm) and "2" (614.2 nm) under 1 mW 532 nm laser excitation. The spectrum, acquired for 10 s, is normalized to 0.5 s for comparison. d) After hours of exposure in 532 nm laser beam at a power of 1 mW, the emitter finally shows two emission peaks at 603.5 and 614.4 nm. The spectrum acquired for 10 s is normalized to 0.5 s for comparison.

3. Discussions

Finally, we briefly discuss the nature of our observations. Considering the emission was observed in germanium implanted diamond, however, the main line is far from the 602 nm and does not exhibit the natural four-line splitting. Nevertheless, this could have been a strained GeV center. Indeed, some strained emitters do show broad inhomogeneous distribution and do not always exhibit the four characteristic lines.[21] Additionally, the closeness of the fluorescence lifetime to that of GeV centers found within the same sample[18] also supports this argument. However, we cannot exclude a color center that has been already present in the diamond and activated upon annealing.

Additionally, density functional theory (DFT) calculations on SiV color centers[21,28] show that it is thermodynamically stable to have Si complexes like SiV2, SiV:H1, etc., in diamond, which usually exhibit a wide range of redshifted emissions as comparing to conventional SiV^- color centers. This is consistent with our observations here that all three emitters display emissions at wavelengths longer than the conventional GeV^- color centers. In this regard, these emitters could be some Ge complexes.

We notice that the separation between the two blinking states is only several to a few tens of nm, which is smaller than that of NV centers (≈60 nm)[5,29] and SiV centers (≈200 nm),[30] but larger than the separation observed in other 0D objects, such as semiconductor quantum dots.[31] Considering the anticorrelation between the two fluorescent states (Figure 1d) and single-photon emission when including all four peaks (Figure 1c), it is unlikely to have charge transfer between multiple defects as the underlying mechanism.

Previous studies on NV color centers associate the blinking and spectral diffusion to the charge dynamics within the emitter itself or the nearby charge traps, especially those at the surface of nanostructures.[32] But since we mainly collect the PL from the center of a solid immersion lens (SIL) that is >2 µm in the diamond, the surface traps can barely affect the emitters. Other possibilities could be the local Fermi level fluctuations due to the ionization or deionization of nearby charge traps, such as P1 centers. In fact, the energy of 532 nm laser is high enough to ionize these centers in the diamond. The disappearance of spectral jumps after high-power exposure might relate to the "permanent" modification of local Fermi level via strain relaxations such that the new configuration of the emitter acquires some robustness against the local environmental instabilities.

Finally, we point out that polarization dependence of each spectral line of states A and B will help clarify the causes for the different emission intensities of states A and B who share a similar radiative lifetime. These measurements along with detailed investigations of exposure effect should provide extra insightful perspectives on the nature of the emitter, which definitely worth additional experimental efforts in the future.

4. Conclusions

In conclusion, we demonstrate the spectral jumps of quantum emitters in diamond under either incoherent and coherent excitation. We show that the spectral jump is a ubiquitous phenomenon that presents in various quantum emitters in diamond. The power dependence of the jumping process suggests the photoinduced ionization process as the possible cause for the phenomenon. Fluorescence blinking is a detrimental effect to quantum information processing, which could be overcome by exposing the quantum emitter to an intense laser beam (see Figure 4 and Figure S2, Supporting Information) or by local Fermi level engineering. The latter is usually achieved by coimplanting different dopants into the material in a cautious manner so as to pin the Fermi level in favor of one charge state, as demonstrated on NV centers[33] and SiV centers[30] in diamond.

5. Experimental Section

Sample Description: The sample is a type-IIa electronic-grade diamond ([N] < 1 ppb), implanted with germanium ions. The diamond substrate was first cleaned with hot Piranha acid for 1 h before fabricating of hemispherical (R = 2.5 µm) SIL on the surface by using focused ion (Ga^+) beam milling (7 nA flux at 30 keV). The SIL microstructure is expected to provide 3–5-folds enhancement for fluorescence collection efficiency. Afterward, Ge^{4+} ions with 7 MeV energy were implanted into SILs followed by a 2 h postannealing at 900 °C in vacuum (2×10^{-6} hPa), leading to a final yield of ≈2–3 emitters per implantation site.

Experimental Setup: The sample was mounted on a XYZ piezo-stepper housed in a 4 K cryostat. A home-built confocal microscope with "NA" = 0.9 is used to address the emitters by using 532 nm diode laser, as shown in Figure 1a. The fluorescence of the sample was collected by using a single-mode optical fiber and directed to a spectrometer for PL spectra characterizations or to avalanche photon diodes (APDs) for time-tagged measurements. The laser scattering was suppressed by passing through long-pass and bandpass optical filters.

Supporting Information

Supporting Information is available from the Wiley Online Library or from the author.

Acknowledgements

Z.M., Y.Z., and D.C. contributed equally to this work. The authors acknowledge Singapore NRF QEP grant, Singapore Ministry of Education (MOE2016-T2-2-077, MOE2016-T2-1-163, and MOE2016-T3-1-006 (S)), A*Star QTE programme, Science Challenge Project (No. TZ2018004), the Australian Research council (via DP180100077), the Asian Office of Aerospace Research and Development grant FA2386-20-1-4014, the Office of Naval Research Global (N62909-18-1-2025), and the AFAiiR node of the NCRIS Heavy Ion Capability for access to ion-implantation/ion-beam analysis facilities.

Conflict of Interest

The authors declare no conflict of interest.

Keywords

binary jumps, single photon emitters

Received: March 23, 2020
Revised: June 25, 2020
Published online: July 15, 2020

[1] a) I. Aharonovich, D. Englund, M. Toth, *Nat. Photonics* **2016**, *10*, 631; b) D. D. Awschalom, R. Hanson, J. Wrachtrup, B. B. Zhou, *Nat. Photonics* **2018**, *12*, 516.

[2] a) G. Kucsko, P. C. Maurer, N. Y. Yao, M. Kubo, H. J. Noh, P. K. Lo, H. Park, M. D. Lukin, *Nature* **2013**, *500*, 54; b) D. M. Toyli, C. F. de las Casas, D. J. Christle, V. V. Dobrovitski, D. D. Awschalom, *Proc. Natl. Acad. Sci. USA* **2013**, *110*, 8417.

[3] M. Atatüre, D. Englund, N. Vamivakas, S.-Y. Lee, J. Wrachtrup, *Nat. Rev. Mater.* **2018**, *3*, 38.

[4] a) T. D. Ladd, F. Jelezko, R. Laflamme, Y. Nakamura, C. Monroe, J. L. O'Brien, *Nature* **2010**, *464*, 45; b) J. R. Weber, W. F. Koehl, J. B. Varley, A. Janotti, B. B. Buckley, C. G. Van de Walle, D. D. Awschalom, *Proc. Natl. Acad. Sci. USA* **2010**, *107*, 8513.

[5] M. W. Doherty, N. B. Manson, P. Delaney, F. Jelezko, J. Wrachtrup, L. C. L. Hollenberg, *Phys. Rep.* **2013**, *528*, 1.

[6] P. Tamarat, T. Gaebel, J. R. Rabeau, M. Khan, A. D. Greentree, H. Wilson, L. C. Hollenberg, S. Prawer, P. Hemmer, F. Jelezko, J. Wrachtrup, *Phys. Rev. Lett.* **2006**, *97*, 083002.

[7] H. Bernien, L. Childress, L. Robledo, M. Markham, D. Twitchen, R. Hanson, *Phys. Rev. Lett.* **2012**, *108*, 043604.

[8] G. Davies, *J. Phys. C: Solid State Phys.* **1974**, *7*, 3797.

[9] P. Tamarat, N. B. Manson, J. P. Harrison, R. L. McMurtrie, A. Nizovtsev, C. Santori, R. G. Beausoleil, P. Neumann, T. Gaebel, F. Jelezko, P. Hemmer, J. Wrachtrup, *New J. Phys.* **2008**, *10*, 045004.

[10] E. Neu, D. Steinmetz, J. Riedrich-Möller, S. Gsell, M. Fischer, S. Matthias, C. Becher, *New J. Phys.* **2011**, *13*, 025012.

[11] a) T. Iwasaki, F. Ishibashi, Y. Miyamoto, Y. Doi, S. Kobayashi, T. Miyazaki, K. Tahara, K. D. Jahnke, L. J. Rogers, B. Naydenov, F. Jelezko, S. Yamasaki, S. Nagamachi, T. Inubushi, N. Mizuochi, M. Hatano, *Sci. Rep.* **2015**, *5*, 12882; b) Y. N. Palyanov, I. N. Kupriyanov, Y. M. Borzdov, N. V. Surovtsev, *Sci. Rep.* **2015**, *5*, 14789.

[12] D. D. Sukachev, A. Sipahigil, C. T. Nguyen, M. K. Bhaskar, R. E. Evans, F. Jelezko, M. D. Lukin, *Phys. Rev. Lett.* **2017**, *119*, 223602.

[13] a) L. J. Rogers, K. D. Jahnke, T. Teraji, L. Marseglia, C. Muller, B. Naydenov, H. Schauffert, C. Kranz, J. Isoya, L. P. McGuinness, F. Jelezko, *Nat. Commun.* **2014**, *5*, 4739; b) S. D. Tchernij, T. Lühmann, T. Herzig, J. Küpper, A. Damin, S. Santonocito, M. Signorile, P. Traina, E. Moreva, F. Celegato, S. Pezzagna, I. P. Degiovanni, P. Olivero, M. Jakšić, J. Meijer, P. M. Genovese, J. Forneris, *ACS Photonics* **2018**, *5*, 4864; c) R. E. Evans, M. K. Bhaskar, D. D. Sukachev, C. T. Nguyen, A. Sipahigil, M. J. Burek, B. Machielse, G. H. Zhang, A. S. Zibrov, E. Bielejec, H. Park, M. Loncar, M. D. Lukin, *Science* **2018**, *362*, 662; d) M. E. Trusheim, B. Pingault, N. H. Wan, M. Gundogan, L. De Santis, R. Debroux, D. Gangloff, C. Purser, K. C. Chen, M. Walsh, J. J. Rose, J. N. Becker, B. Lienhard, E. Bersin, I. Paradeisanos, G. Wang, D. Lyzwa, A. R. Montblanch, G. Malladi, H. Bakhru, A. C. Ferrari, I. A. Walmsley, M. Atature, D. Englund, *Phys. Rev. Lett.* **2020**, *124*, 023602; e) J. L. Zhang, S. Sun, M. J. Burek, C. Dory, Y. K. Tzeng, K. A. Fischer, Y. Kelaita, K. G. Lagoudakis, M. Radulaski, Z. X. Shen, N. A. Melosh, S. Chu, M. Loncar, J. Vuckovic, *Nano Lett.* **2018**, *18*, 1360; f) C. Bradac, W. Gao, J. Forneris, M. E. Trusheim, I. Aharonovich, *Nat. Commun.* **2019**, *10*, 5625.

[14] a) C. Hepp, T. Muller, V. Waselowski, J. N. Becker, B. Pingault, H. Sternschulte, D. Steinmuller-Nethl, A. Gali, J. R. Maze, M. Atature, C. Becher, *Phys. Rev. Lett.* **2014**, *112*, 036405; b) M. K. Bhaskar, D. D. Sukachev, A. Sipahigil, R. E. Evans, M. J. Burek, C. T. Nguyen, L. J. Rogers, P. Siyushev, M. H. Metsch, H. Park, F. Jelezko, M. Loncar, M. D. Lukin, *Phys. Rev. Lett.* **2017**, *118*, 223603.

[15] A. Sipahigil, K. D. Jahnke, L. J. Rogers, T. Teraji, J. Isoya, A. S. Zibrov, F. Jelezko, M. D. Lukin, *Phys. Rev. Lett.* **2014**, *113*, 113602.

[16] a) P. Frantsuzov, M. Kuno, B. Jankó, R. A. Marcus, *Nat. Phys.* **2008**, *4*, 519; b) C. Bradac, T. Gaebel, N. Naidoo, M. J. Sellars, J. Twamley, L. J. Brown, A. S. Barnard, T. Plakhotnik, A. V. Zvyagin, J. R. Rabeau, *Nat. Nanotechnol.* **2010**, *5*, 345.

[17] a) P. Siyushev, V. Jacques, I. Aharonovich, F. Kaiser, T. Müller, L. Lombez, M. Atatüre, S. Castelletto, S. Prawer, F. Jelezko, J. Wrachtrup, *New J. Phys.* **2009**, *11*, 113029; b) T. Müller, I. Aharonovich, L. Lombez, Y. Alaverdyan, A. N. Vamivakas, S. Castelletto, F. Jelezko, J. Wrachtrup, S. Prawer, M. Atatüre, *New J. Phys.* **2011**, *13*, 075001; c) N. Aslam, G. Waldherr, P. Neumann, F. Jelezko, J. Wrachtrup, *New J. Phys.* **2013**, *15*, 013064; d) M. Berthel, O. Mollet, G. Dantelle, T. Gacoin, S. Huant, A. Drezet, *Phys. Rev. B* **2015**, *91*, 035308; e) S. Dhomkar, P. R. Zangara, J. Henshaw, C. A. Meriles, *Phys. Rev. Lett.* **2018**, *120*, 117401.

[18] D. Chen, Z. Mu, Y. Zhou, J. E. Froch, A. Rasmit, C. Diederichs, N. Zheludev, I. Aharonovich, W. B. Gao, *Phys. Rev. Lett.* **2019**, *123*, 033602.

[19] a) C. Galland, Y. Ghosh, A. Steinbrück, M. Sykora, J. A. Hollingsworth, V. I. Klimov, H. Htoon, *Nature* **2011**, *479*, 203; b) A. L. Efros, D. J. Nesbitt, *Nat. Nanotechnol.* **2016**, *11*, 661.

[20] a) R. E. Evans, A. Sipahigil, D. D. Sukachev, A. S. Zibrov, M. D. Lukin, *Phys. Rev. Appl.* **2016**, *5*, 044010; b) P. Siyushev, M. H. Metsch, A. Ijaz, J. M. Binder, M. K. Bhaskar, D. D. Sukachev, A. Sipahigil, R. E. Evans, C. T. Nguyen, M. D. Lukin, *Phys. Rev. B* **2017**, *96*, 081201.

[21] S. Lindner, A. Bommer, A. Muzha, A. Krueger, L. Gines, S. Mandal, O. Williams, E. Londero, A. Gali, C. Becher, *New J. Phys.* **2018**, *20*, 115002.

[22] C. P. Anderson, A. Bourassa, K. C. Miao, G. Wolfowicz, P. J. Mintun, A. L. Crook, H. Abe, J. U. Hassan, N. T. Son, T. Ohshima, *Science* **2019**, *366*, 1225.

[23] a) J. Dreiser, M. Atatüre, C. Galland, T. Müller, A. Badolato, A. Imamoglu, *Phys. Rev. B* **2008**, *77*, 075317; b) C. F. de las Casas,

D. J. Christle, J. Ul Hassan, T. Ohshima, N. T. Son, D. D. Awschalom, *Appl. Phys. Lett.* **2017**, *111*, 262403.
[24] R. J. Cook, H. J. Kimble, *Phys. Rev. Lett.* **1985**, *54*, 1023.
[25] X. Chen, C. Zou, Z. Gong, C. Dong, G. Guo, F. Sun, *Light: Sci. Appl.* **2015**, *4*, e230.
[26] P. Siyushev, H. Pinto, M. Vörös, A. Gali, F. Jelezko, J. Wrachtrup, *Phys. Rev. Lett.* **2013**, *110*, 167402.
[27] a) H. Sternschulte, K. Thonke, R. Sauer, P. C. Munzinger, P. Michler, *Phys. Rev. B* **1994**, *50*, 14554; b) E. Neu, C. Hepp, M. Hauschild, S. Gsell, M. Fischer, H. Sternschulte, D. Steinmüller-Nethl, M. Schreck, C. Becher, *New J. Phys.* **2013**, *15*, 043005.
[28] G. Thiering, A. Gali, *Phys. Rev. B* **2015**, *92*, 165203.
[29] N. B. Manson, J. P. Harrison, M. J. Sellars, *Phys. Rev. B* **2006**, *74*, 104303.
[30] B. C. Rose, D. Huang, Z. H. Zhang, P. Stevenson, A. M. Tyryshkin, S. Sangtawesin, S. Srinivasan, L. Loudin, M. L. Markham, A. M. Edmonds, D. J. Twitchen, S. A. Lyon, N. P. de Leon, *Science* **2018**, *361*, 60.
[31] R. J. Warburton, *Nat. Mater.* **2013**, *12*, 483.
[32] L. Rondin, G. Dantelle, A. Slablab, F. Grosshans, F. Treussart, P. Bergonzo, S. Perruchas, T. Gacoin, M. Chaigneau, H. C. Chang, V. Jacques, J. F. Roch, *Phys. Rev. B* **2010**, *82*, 115449.
[33] F. Favaro de Oliveira, D. Antonov, Y. Wang, P. Neumann, S. A. Momenzadeh, T. Haussermann, A. Pasquarelli, A. Denisenko, J. Wrachtrup, *Nat. Commun.* **2017**, *8*, 15409.